Role of Tryptophan-74 of the Recombinant Kringle 2 Domain of Tissue-Type Plasminogen Activator in Its ω-Amino Acid Binding Properties†

Vesna S. De Serrano and Francis J. Castellino*

Department of Chemistry and Biochemistry, University of Notre Dame, Notre Dame, Indiana 46556

Received October 21, 1991; Revised Manuscript Received January 14, 1992

ABSTRACT: The role of W^{74} in stabilization of the binding of ω-amino acids to the recombinant (r) kringle 2 domain (residues 180–261) of tissue-type plasminogen activator ([$K2_{tPA}$]) has been assessed by examination of the binding (dissociation) constants (K_d) of ε-aminocaproic acid (EACA) and one of its structural analogues, 7-aminoheptanoic acid (7-AHpA), to variants of r-[$K2_{tPA}$] generated by site-directed mutagenesis of the wild-type kringle domain. Two nonconservative mutations at W^{74} of r-[$K2_{tPA}$] have been constructed, expressed, and purified, resulting in one variant molecule containing a $W^{74}L$ mutation (r-[$K2_{tPA}/W^{74}L$]) and another containing a $W^{74}S$ mutation (r-[$K2_{tPA}/W^{74}S$]). In both cases, binding of EACA and 7-AHpA was virtually eliminated in the mutated kringles. Two additional conservative mutations at W^{74} of r-[$K2_{tPA}$] have been similarly generated, resulting in r-[$K2_{tPA}/W^{74}F$] and r-[$K2_{tPA}/W^{74}Y$]. For these mutants, binding of the same ligands to the variant recombinant kringle domain is retained, although it is significantly weaker in nature. The ^{1}H-NMR spectra of each of the variant kringles demonstrates that all retain the general gross conformations of their wild-type counterpart but that some environmental changes of proton resonances occur at particular aromatic amino acid residues that may be involved in ω-amino acid binding. Differential scanning calorimetric analyses of each of the variant kringles suggest that none of the mutations led to substantial destabilization of their structures, again suggestive of gross conformational similarities in all r-[$K2_{tPA}$] molecules constructed. We conclude that the aromatic character present at position 74 of wild-type r-[$K2_{tPA}$] is of great importance to its ability to interact with ω-amino acid ligands, with tryptophan being the most effective amino acid at that position.

Kringles are triple disulfide-bonded highly homologous regions of proteins that contain approximately 80 amino acids (Magnusson et al., 1975). Such structures have been found in a variety of proteins, several of which contain multiple copies. For example, one kringle is found in coagulation factor XII (McMullen & Fujikawa, 1985) and in urokinase (Steffens et al., 1982), two kringles have been located in tPA[1] (Pennica et al., 1983) and prothrombin (Magnusson et al., 1975), five kringles exist in HPg (Sottrup-Jensen et al., 1978), and a total of 38 kringles are present in apolipoprotein(*a*) (McLean et al., 1987).

The exact functions of the kringles are not fully understood, yet these domains have been shown to be of importance in the regulatory properties of several of the above proteins. Among their most well-established roles includes the ability of antifibrinolytic ω-amino acids, typified by L-lysine and EACA, to interact with kringles of HPg (Markus et al., 1978a,b; Sottrup-Jensen et al., 1978; Thewes et al., 1987; Sehl & Castellino, 1990; Menhart et al., 1991) and tPA (van Zonneveld et al., 1986; Cleary et al., 1989). Kringles also contain binding sites for fibrin to HPg (Thorsen, 1975; Wiman & Wallen, 1977; Thorsen et al., 1981) and tPA (van Zonneveld et al., 1986; de Munk et al., 1989), as well as binding sites for α_2-antiplasmin to HPm (Wiman & Collen, 1978). It also appears as though the kringle 1–3 region of HPg plays an important role in the binding of HPg to platelets (Miles et al., 1988).

While the kringle regions of these proteins are highly homologous, they do not possess identical functional properties. For example, it has been demonstrated that [$K1_{HPg}$] (Lerch et al., 1980; Menhart et al., 1991), [$K4_{HPg}$] (Lerch et al., 1980; DeMarco et al., 1987, 1989; Sehl & Castellino, 1990), [$K5_{HPg}$] (Castellino et al., 1981; DeMarco et al., 1985; Novokhatny et al., 1989; Thewes et al., 1990), and [$K2_{tPA}$] (Cleary et al., 1989) interact with ω-amino acids, whereas such binding has not been demonstrated to occur with [$K2_{HPg}$], [$K3_{HPg}$], [$K1_{tPA}$], [K_{UK}], [$K1_{PT}$], or [$K2_{PT}$]. The nature of the ω-amino acid binding site of the relevant kringle domains has been the subject of intense study because this interaction has been implicated in most of the functional binding properties of these domains. On the basis of earlier chemical modification studies, it was suggested that D^{56} and R^{69} of [$K4_{HPg}$] formed ion-pair interactions with the complementary functional groups of

†Supported by Grant HL-13423 from the National Institutes of Health, Grant 89/833 from the American Heart Association, and the Kleiderer/Pezold family endowed professorship (to F.J.C.).

* To whom to address correspondence.

[1] Abbreviations: tPa, tissue-type plasminogen activator; HPg, human plasminogen; HPm, human plasmin; [$K1_{HPg}$], the kringle 1 region (residues C^{84}–C^{162}) of human plasminogen; [$K2_{HPg}$], the kringle 2 region (residues C^{166}–C^{243}) of human plasminogen; [$K3_{HPg}$], the kringle 3 region (residues C^{256}–C^{333}) of human plasminogen; [$K4_{HPg}$], the kringle 4 region (residues C^{358}–C^{435}) of human plasminogen; [$K5_{HPg}$], the kringle 5 region (residues C^{462}–C^{541}) of human plasminogen; [$K1_{tPA}$], the kringle 1 region (residues C^{92}–C^{173}) of human tissue-type plasminogen activator; [$K2_{tPA}$], the kringle 2 region (residues C^{180}–C^{261}) of human tissue-type plasminogen activator; [$K2_{tPA}/W^{74}X$], the kringle 2 region (residues C^{180}–C^{261}) of human tissue-type plasminogen activator with W^{74} altered to the amino acid immediately following (represented by X); [K_{UK}], the kringle region (residues C^{50}–C^{131}) of human urokinase; [$K1_{PT}$], the kringle 1 region (residues C^{65}–C^{143}) of human prothrombin; [$K2_{PT}$], the kringle 2 region (residues C^{170}–C^{248}) of human prothrombin; [K_{fXII}], the kringle region (residues C^{198}–C^{276}) of human factor XII; P_{fXa}, a peptide (IEGR′SX_n) which is predicted to be sensitive to cleavage, at the R′S peptide bond, by factor Xa; EACA, ε-aminocaproic acid; phoA, alkaline phosphatase, bp, base pair; r, recombinant; wt, wild type; PCR, polymerase chain reaction; NaDodSO$_4$/PAGE, sodium dodecyl sulfate/polyacrylamide gel electrophoresis; FPLC, fast protein liquid chromatography; DSC, differential scanning calorimetry.

0006-2960/92/0431-3326$03.00/0

EACA (Trexler et al., 1982), although this same cationic binding center in [$K1_{HPg}$] has also been proposed to include R^{32} and R^{34} (Vali & Patthy, 1984). In [$K2_{tPA}$], results from molecular modeling studies have suggested that D^{57} and H^{65} contribute the anionic and cationic centers for binding of ω-amino acids (Tulinsky et al., 1988). However, binding studies utilizing recombinant H^{65}-variant forms of r-[$K2_{tPA}$] have led to results that have eliminated that amino acid residue as an essential cation for ω-amino acid ligand binding (Kelley & Cleary, 1989). Site-directed mutagenesis studies in our laboratory with [$K2_{tPA}$] have directly implicated K^{33} as the principal cationic center for interaction of this kringle domain with ω-amino acids (De Serrano et al., 1991). In addition to the important ion-pair interactions, ^{1}H-NMR investigations have shown that aromatic residues in HPg kringles (Motta et al., 1986; Ramesh et al., 1987; Tulinsky et al., 1988; Thewes et al., 1990), as well as in [$K2_{tPA}$], are perturbed by addition of ω-amino acids to these domains. In [$K2_{tPA}$], the aromatic residues believed to be important in this regard include W^{25}, W^{63}, H^{65}, W^{74}, and Y^{76} (Byeon et al., 1989).

The crystal structure of r-[$K2_{tPA}$] has been determined. Fortuitously, the unit cell contained the side chain of K^{49} from one r-[$K2_{tPA}$] molecule inserted into the ω-amino acid binding pocket of a second r-[$K2_{tPA}$] molecule (de Vos et al., 1992). It appears from the structure that of great importance to this binding site is the binding stabilization provided by interaction of the side chain of W^{74} with the hydrophobic backbone of the lysine side chain occupying the binding site. While the structure in hand[2] is an excellent starting point for detailed molecular understanding of the [$K2_{tPA}$]/ω-amino acid interactions, it suffers from some limitations. Specifically, the X-ray crystal structure may differ from the solution structure due to lattice energy stabilization forces in the crystal state that do not exist in solution, and these considerations may influence binding site residue relationships. Further, the unit cell was crystallized as a trimer of r-[$K2_{tPA}$], and the conformation of its binding site may have been affected by interkringle interactions. Finally, the crystallized r-[$K2_{tPA}$] has the ω-amino acid ligand binding site occupied, not with free ligand but with a lysine side chain from another r-[$K2_{tPA}$] domain. Thus, this latter interaction is absent the stabilization that would be provided if the carboxy group of the ligand were also available for binding, and this may have affected the positioning of the ligand in the binding site. We have designed a program to test the molecular details of the ligand/[$K2_{tPA}$] interaction in solution by site-directed mutagenesis of key residues predicted to be of importance to ω-amino acid binding and also of residues that are important to maintenance of the structural integrity of this kringle. This paper summarizes results of our detailed investigation of the important role of W^{74} in structure–function properties of r-[$K2_{tPA}$].

Materials and Methods

Proteins. Bovine fXa was donated by Enzyme Research Laboratories, Inc. (South Bend, IN). Recombinant Taq DNA polymerase (AmpliTaq) was obtained from Perkin-Elmer Cetus (Norwalk, CT). Restriction endonucleases were purchased from Fisher Scientific Co. (Springfield, NJ) and BRL (Gaithersberg, MD).

Plasmids. The plasmid phGH4R, previously employed for expression of human growth factor, contains the phoA promoter and the heat-stable enterotoxin (stII) signal sequence (Chang et al., 1987). The construction of plasmid pUC118-tPA, containing the wild-type tPA sequence in pUC118, has been described (De Serrano & Castellino, 1990). The method of construction of the *Escherichia coli* fusion expression vector p[$K1_{HPg}$]P_{fXa}, the essential features of which are summarized below, is described in a forthcoming publication (De Serrano et al., 1992).

Construction of the Expression Vector pSTII[$K2_{tPA}$]. Details of the construction of the *E. coli* expression plasmid, coding for r-SD[$K2_{tPA}$]S, have been described (De Serrano et al., 1991).

Construction of the Fusion Protein Expression Plasmids p[$K1_{HPg}$]P_{fXa}[$K2_{tPA}/W^{74}S$] and p[$K1_{HPg}$]P_{fXa}[$K2_{tPA}/W^{74}L$]. The starting plasmids were pSTII[$K2_{tPA}$] and p[$K1_{HPg}$]P_{fXa}. This latter *E. coli* fusion protein expression plasmid consists of the phoA promoter and the stII signal sequence to drive transcription and secretion, respectively. In-frame with, and immediately downstream of, the signal sequence is a cDNA encoding the tight lysine-binding [$K1_{HPg}$] region (Menhart et al., 1991), followed by a peptide domain (P_{fXa}) that forms a recognition site for the serine protease factor Xa. Downstream of this region are *Bst*XI and *Sal*I sites within which the target molecule is placed, in-frame with the factor Xa recognition sequence.

The coding sequence of W^{74} in tPA, in pSTII[$K2_{tPA}$], was mutated to the coding sequences of S^{74} and L^{74}. For the $W^{74}S$ mutation, the primer (the mutagenic bases are represented by lower-case lettering)

5′-C AGG CTG ACG Tct GAG TAC TGT GA

was employed. Mutant colonies were identified by the newly created restriction endonuclease site for *Aat*II, present after base 11 of the above primer. This resulted in isolation of plasmid pSTII[$K2_{tPA}/W^{74}S$].

The cDNA containing the nucleotide sequence coding for SD[$K2_{tPA}/W^{74}S$]S was cleaved with *Nsi*I/*Sal*I from plasmid pSTII[$K2_{tPA}/W^{74}S$], and the resulting 0.266-kb fragment was purified as above. This cDNA was inserted into the *Bst*XI/*Sal*I sites of p[$K1_{HPg}$]P_{fXa}, yielding p[$K1_{HPg}$]P_{fXa}-[$K2_{tPA}/W^{74}S$], which was expressed in *E. coli* DH5α cells as described (De Serrano et al., 1991). After translation and subsequent cleavage of the signal sequence, a fusion polypeptide results, containing the amino acid sequence SE-[$K1_{HPg}$]DIEGR′SNASD[$K2_{tPA}/W^{74}S$]S. Catalytic cleavage of the R′S peptide bond with factor Xa leads to liberation of the target molecule r-SNASD[$K2_{tPA}/W^{74}S$]S.

The following synthetic oligonucleotide mutagenic primer was employed to alter the W^{74} codon in pSTII[$K2_{tPA}$] to L^{74}:

5′-C CGC AGG CTG ACa ctG GAG TAC TGT GA

Positive transformants were identified by the existence of a newly created restriction endonuclease site for *Bsr*I, present after base 13 in the above primer. All subsequent steps for construction of the fusion polypeptide expression plasmid p[$K1_{HPg}$]P_{fXa}[$K2_{tPA}/W^{74}L$] were as above. After expression, and subsequent cleavage with factor Xa, the target molecule contained the amino acid sequence r-SNASD[$K2_{tPA}/W^{74}L$]S.

Construction of the Expression Vectors pSTII[$K2_{tPA}/W^{74}F$] and pSTII[$K2_{tPA}/W^{74}Y$]. For these variants, we employed the mutant pSTII[$K2_{tPA}/W^{74}L$] as the starting plasmid, and screened positive transformants for the loss of the *Bsr*I restriction endonuclease site that was previously cloned into the plasmid concomitant with the $W^{74}L$ mutation.

In order to obtain the $L^{74}F$ mutation, the mutagenic primer (the mutated nucleotides in this section are referenced to [$K2_{tPA}/W^{74}L$])

[2] The coordinates were provided to this laboratory by Dr. A. M. de Vos, Genentech, Inc., South San Francisco, CA.

5′-CGC AGG CTG ACA tTc GAG TAC TGT GAT

was annealed to the noncoding strand of pSTII[$K2_{tPA}/W^{74}L$]. This resulted in construction of plasmid pSTII[$K2_{tPA}/W^{74}F$] (although the L^{74} mutant was employed as the starting material for the mutation, we nonetheless named the plasmid and the resulting protein as representing an alteration from W^{74}, which is the residue at that location in wild-type r-[$K2_{tPA}$]). This plasmid was directly expressed in *E. coli* DH5α cells, according to the procedure previously published (Menhart et al., 1991). After cleavage of the signal polypeptide, the relevant gene product consisted of the amino acid sequence r-SD[$K2_{tPA}/W^{74}F$]S.

Similarly, for construction of the $L^{74}Y$ mutant, the primer

5′-CGC AGG CTG ACA tac GAG TAC TGT GAT

was annealed to the noncoding strand of pSTII[$K2_{tPA}/W^{74}L$]. This led to isolation of plasmid pSTII[$K2_{tPA}/W^{74}Y$], which was directly expressed as above for wtr-[$K2_{tPA}$]. This plasmid, after cleavage of the signal polypeptide, codes for an amino acid sequence of r-SD[$K2_{tPA}/W^{74}Y$]S.

DNA Analytical Methods. Oligonucleotides were synthesized on a Biosearch (San Rafael, CA) Cyclone two-column DNA synthesizer using phosphoramidite methodology. The resulting oligonucleotides were purified using Applied Biosystems (Foster City, CA) oligonucleotide purification cartridges. cDNAs were sequenced by the dideoxy technique (Sanger et al., 1977) using the Sequenase reagent kit (U.S. Biochemicals, Cleveland, OH). Cell transformations were accomplished using the calcium phosphate/$RbCl_2$ method (Kurecki et al., 1979; Seidman, 1987). Plasmid minipreparations were obtained by the alkaline lysate method (Lech & Brent, 1987).

Single-strand plasmid DNAs were generated by the method of Vieira and Messing (1987). The cDNAs and cDNA fragments were purified after their electrophoretic separation on a suitable concentration of agarose, using the Geneclean kit (BIO 101, Inc., La Jolla, CA).

PCR amplifications of DNA were conducted by employing a Perkin-Elmer Cetus DNA thermal cycler, with all reagents purchased from Perkin-Elmer Cetus. Temperature cycling conditions used for the PCR were as follows: melting for 60 s at 94 °C; annealing for 60 s at 45 °C, extension by ramping to 72 °C over 60 s, followed by an additional 60 s at this temperature. The reaction (25 cycles) was carried out in 100 μL of a solution containing 10 mM Tris-HCl/50 mM KCl/0.001% (w/v) gelatin/2.5 mM $MgCl_2$/0.2 mM deoxynucleotide triphosphates/600 nM desired primers/1 unit of Taq DNA polymerase.

Purification of Recombinant Kringles. Prior to beginning the purification processes, the transformed *E. coli* cells were separated into the cytoplasmic, periplasmic, and oxidatively refolded fractions (Menhart et al., 1991).

Purification of wtr-[$K2_{tPA}$] from the periplasmic and refolded fractions was accomplished by affinity chromatography and FPLC steps as described previously (De Serrano et al., 1991).

In the case of the variants that interacted directly with Sepharose–lysine affinity chromatography columns, viz., r-[$K2_{tPA}/W^{74}F$] and r-[$K2_{tPA}/W^{74}Y$], purification was accomplished in the same manner as above, with an operational modification necessitated by the weaker interactions of r-[$K2_{tPA}/W^{74}F$] and r-[$K2_{tPA}/W^{74}Y$] to Sepharose–lysine. In these cases, the Sepharose–lysine column was washed with a lower salt buffer (50 mM phosphate, pH 7.4) than was used for this same chromatography step with wtr-[$K2_{tPA}$], prior to elution of the variant kringles with EACA (Menhart et al., 1991). Upon subsequent dialysis against the starting buffer for the FPLC step, a precipitate formed, which was found to contain the bulk of the impurities and virtually no kringle material. Thus, the precipitates were discarded. FPLC was then conducted as above, with essentially the same elution position observed for both variants.

For the variants that did not directly interact with Sepharose–lysine, viz., the $W^{74}L$ and $W^{74}S$ variants, the tandem kringles r-SE[$K1_{HPg}$]DIEGR′SNASD[$K2_{tPA}/W^{74}L$]S and r-SE[$K1_{HPg}$]DIEGR′SNASD[$K2_{tPA}/W^{74}S$]S were purified by affinity chromatography on Sepharose–lysine and FPLC, as above. Next, the mutant kringles r-[$K2_{tPA}/W^{74}L$] and r-[$K2_{tPA}/W^{74}S$] were liberated from the tandem kringle construction by cleavage with factor Xa, and the r-[$K1_{HPg}$] portion was removed by its adsorption to a Sepharose–lysine affinity column. Final purifications of r-[$K2_{tPA}/W^{74}S$] and r-[$K2_{tPA}/W^{74}L$], both of which passed unretarded through the second Sepharose–lysine column, were accomplished by FPLC as above. Only minor differences in elution behavior on FPLC for these latter kringles were observed.

^{1}H-NMR Spectroscopy. Samples for NMR were prepared by dissolution of the lyophilized peptide in 0.05 M phosphate, pH 7.4 (fully preexchanged with ^2H_2O), lyophilization of the sample, and dissolution in the same volume of ^2H_2O two additional times for nearly complete ^1H–^2H exchange.

One-dimensional ^{1}H-NMR spectra were recorded at 37 °C on a Varian (Palo Alto, CA) VXR 500S spectrometer in the Fourier mode at 500 MHz with quadrature detection. The spectral width was 6000 Hz and the number of data points was 64 000, providing a digital resolution of 0.19 Hz. Suppression of the residual $^1H^2HO$ peak was accomplished by gated pulse irradiation of this resonance at low decoupling power for 1.5 s between scans. The chemical shifts (ppm) reported are relative to an internal standard of dioxane, which resonates 3.77 ppm downfield of tetramethylsilane. Enhancement of the resolution was achieved by Gaussian convolution.

Two-dimensional RELAYED-COSY spectra were obtained at 37 °C by employing the computer software programs provided by the Varian Company for pulse sequences, spectral deconvolution, and data presentation. The pulse sequence employed was 1.5-s (saturation of residual $^1H^2HO$)–90°–t_1–90°–τ/2–180°–τ/2–90°–t_2 (Eich et al., 1982). The spectral width was 5448 Hz, with a block size of 2048 data points. A total of 256 time increments and 128 transients for each time increment were collected.

Differential Scanning Calorimetry. DSC experiments were conducted with the use of a Microcal (Northampton, MA) MC-2 scanning calorimeter. The sample was dissolved in a solution of 50 mM Tris–OAc/150 mM NaOAc, pH 8.0, or 50 mM Tris–OAc/100 mM NaOAc/50 mM EACA, pH 8.0, and exhaustively dialyzed against the same solution. The material was then added to the sample chamber of the calorimeter, and an identical volume of dialyzate was placed in the reference cell. The chambers were temperature-equilibrated at 20 °C, and the run was initiated. Thermal denaturation scans were conducted between the temperature range of 25–100 °C, at scan rates of 30 °C/h, to obtain the resulting thermograms. The baseline for each run was determined by an identical experiment with the sample buffer placed in each chamber. The information obtained was recorded on an IBM-PC computer for further data reduction.

We have previously described the methods that we employ for deconvolution of the traces and for obtaining the temperature of maximum heat capacity (T_m) and the calorimetric

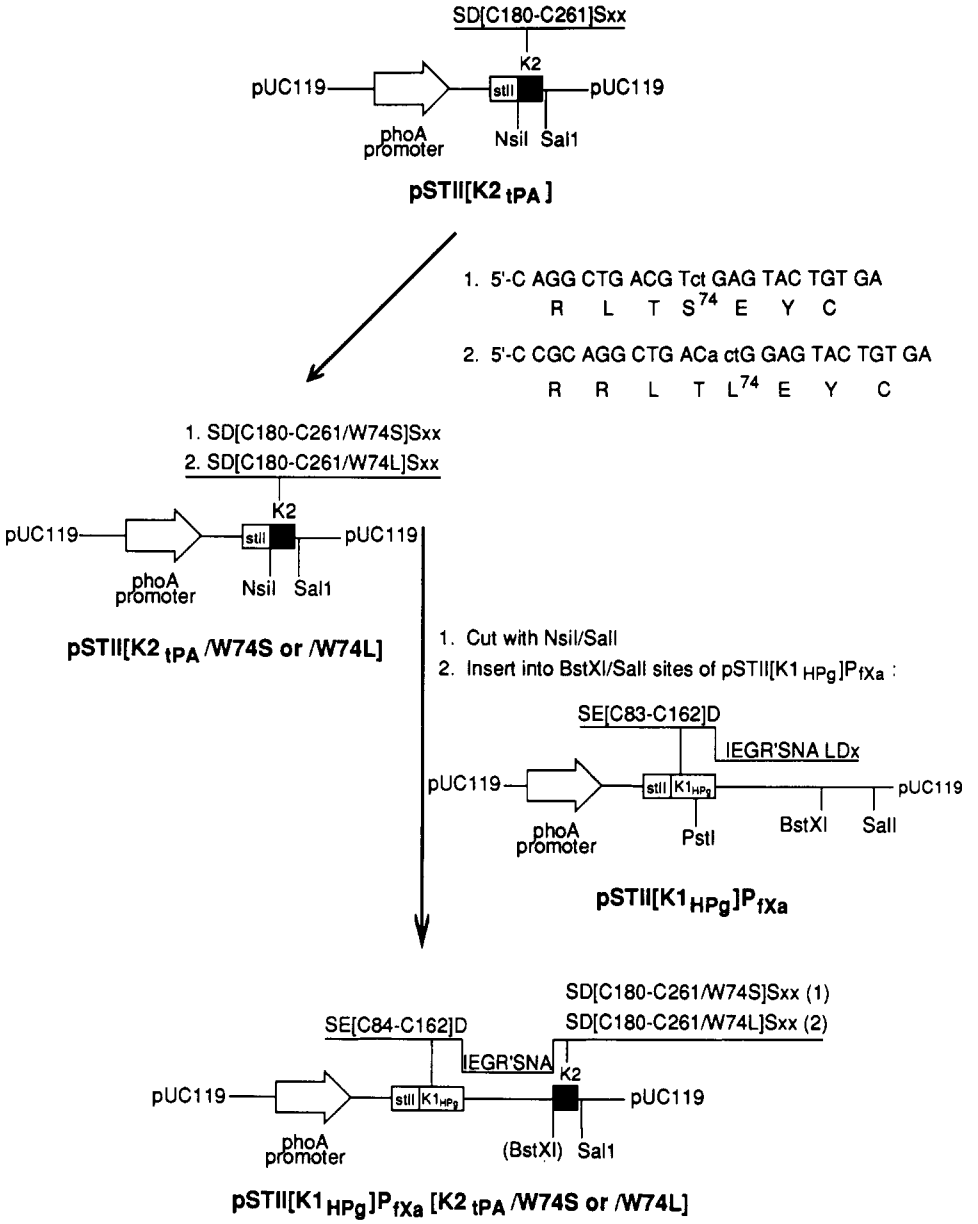

FIGURE 1: Construction of the fusion expression vectors for r-SD[$K2_{tPA}$/W^{74}L]S and r-SD[$K2_{tPA}$/W^{74}S]S. This plasmid was mutagenized with primer 1 or 2 (the lower-case lettering refers to changes from the wild-type cDNA), resulting in plasmids pSTII[$K2_{tPA}$/W^{74}S] and pSTII[$K2_{tPA}$/W^{74}L], which are direct *E. coli* expression vectors for r-SD[$K2_{tPA}$/W^{74}S]S and r-SD[$K2_{tPA}$/W^{74}L]S, respectively. Upon subsequent failure of these expressed kringle variants to interact with the Sepharose–lysine affinity chromatography columns, each mutagenized cDNA was inserted into plasmid pSTII[$K1_{HPg}$]P_{fXa}, providing plasmids pSTII[$K1_{tPA}$/W^{74}L], which yielded the polypeptides r-SE[$K1_{HPg}$]-DIEGR'SNASD[$K2_{tPA}$/W^{74}S]S and r-SE[$K1_{HPg}$]DIEGR'SNASD[$K2_{tPA}$/W^{74}L]S after expression. PhoA refers to the alkaline phosphatase promoter region, stII represents the heat-stable enterotoxin signal sequence, and x symbolizes a stop codon. The factor Xa-sensitive bond in the fusion polypeptide is represented by R'S.

$\Delta H(\Delta H_{cal})$ (Radek & Castellino, 1988). At the scan rate chosen (0.5 °C/min), the T_m was independent of the rate of temperature change.

Intrinsic Fluorescence. Titrations of the effect of ω-amino acids on the intrinsic fluorescence of the recombinant kringles, and calculation of the dissociation constants (K_d) of the kringle/ω-amino acid interactions from these titrations, were accomplished as previously described (Menhart et al., 1991).

Titration Calorimetry. These experiments, designed to measure thermodynamic constants for the binding of ω-amino acids to the r-[$K2_{tPA}$] constructs, were performed essentially as described in previous papers from this laboratory (Sehl & Castellino, 1990; Menhart et al., 1991). The titrations were performed by employing a Microcal (Northampton, MA) OMEGA titration calorimeter at 25 °C and the data evaluated as described (Sehl & Castellino, 1990; Menhart et al., 1991) with the latest software available from this same company. Titrations were conducted in a buffer of 50 mM Tris-OAc/150 mM NaOAc, pH 8.0, at 25 °C.

Protein Analytical Methods. Electrospray–mass spectrographic analysis for determination of the molecular weight of the samples was conducted using a JOEL (Peabody, MA) AX505 gas chromatograph/mass spectrometer equipped with the JOEL electrospray ionization source. $NaDodSO_4$/PAGE was performed as described earlier (Laemmli, 1970).

RESULTS

Two recombinant variants of [$K2_{tPA}$], containing W^{74}L and W^{74}S mutations, have been constructed. These variants were expressed by employing a cleavable fusion plasmid, according to the steps summarized in Figure 1, since neither variant interacted with Sepharose–lysine affinity chromatography

Table I: Molecular Weights of W^{74} Mutants of the Recombinant Kringle 2 Region of Tissue-Type Plasminogen Activator

kringle	mol wt calcd	mol wt exptl
SD[$K2_{tPA}$]S	9365.69	9369.40
SD[$K2_{tPA}/W^{74}F$]S	9326.66	9325.96
SD[$K2_{tPA}/W^{74}Y$]S	9342.66	9342.10
SNASD[$K2_{tPA}/W^{74}S$]S	9538.86	9542.70
SNASD[$K2_{tPA}/W^{74}L$]S	9564.94	9567.50

columns when expressed directly, thus severely complicating the purification process. The fusion plasmids contained the target molecules covalently joined to r-[$K1_{HPg}$], a strong lysine-binding kringle, with an interconnecting peptide region susceptible to cleavage by factor Xa. The tandem kringles were then purified by Sepharose–lysine affinity chromatography and FPLC. Next, the target molecules were liberated by limited proteolysis with factor Xa, and the r-[$K1_{HPg}$] component was removed by virtue of its ability to interact with Sepharose–lysine. The desired r-[$K2_{tPA}$] variants, which passed unretarded through the column after their cleavage from r-[$K1_{HPg}$], were purified by FPLC. Final yields of the variant kringles of 10–15 mg/150 g of cells (wet weight) were obtained. Approximately 1–2 mg was present in the cellular periplasmic fraction, with the remainder in the oxidatively refolded cell-associated materials. Because of the strategy employed for these two variants, the amino acid sequence of SNASD preceded C^1 of the kringle, and S followed the carboxyl-terminal amino acid, C^{82}, in each case. The purified variants displayed single components on $NaDodSO_4$/PAGE with the expected approximate molecular weights. Precise molecular weights were obtained by electrospray mass spectrometry. The results are summarized in Table I and compare very favorably to calculated values for these same two variants. These data clearly demonstrate that the cDNAs were properly translated and processed and that the fused kringles were cleaved by factor Xa, as expected.

Two additional recombinant variants of [$K2_{tPA}$], containing $W^{74}F$ and $W^{74}Y$ mutations, have been constructed and directly expressed in *E. coli* cells. These variants were then isolated and purified by Sepharose–lysine affinity chromatography and FPLC methodology. A summary of the steps involved in construction of the expression vectors for each variant, conveniently employing the $W^{74}L$ variant as the starting material, is provided in Figure 2. In both cases, approximately 3–5 mg/150 g (wet weight) of cells was obtained in the respective periplasmic fractions of cells, and approximately 35–50 mg of each variant was obtained from the corresponding oxidatively refolded cell-associated materials. A similar yield of wtr-[$K2_{tPA}$] was obtained by employing this expression system. By nature of these constructions, wtr-[$K2_{tPA}$], r-[$K2_{tPA}/W^{74}F$], and r-[$K2_{tPA}/W^{74}Y$] possessed a sequence of SD, preceding C^1 of the kringle, and S, following C^{82} of the kringle. In each case, the purified materials contained a single component consistent with the expected molecular weights on reduced $NaDodSO_4$/PAGE gels. Precise molecular weights for these two variant r-[$K2_{tPA}$] constructions were obtained by electrospray mass spectrometry and are listed in Table I. The experimental values are in excellent agreement with those calculated from the amino acid sequences. Again, these results provide clear evidence that each cDNA was correctly translated and processed.

Two methods were employed to measure the dissociation contants (K_d) of ω-amino acid ligands, viz., EACA and 7-AHpA, to the various r-[$K2_{tPA}$] molecules generated in this study. One method takes advantage of the approximate 30%

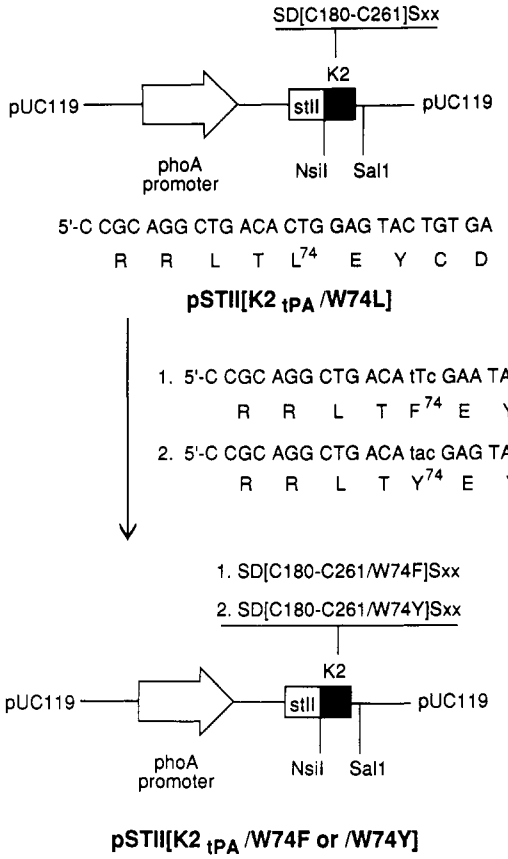

FIGURE 2: Construction of the direct expression vectors for r-SNASD[$K2_{tPA}/W^{74}F$]S and r-SNASD[$K2_{tPA}/W^{74}Y$]S. Plasmid pSTII[$K2_{tPA}/W^{74}L$] (see Figure 1), which is a direct *E. coli* expression vector coding for wtr-SD[$K2_{tPA}/W^{74}L$]S, was used as the starting material. The oligonucleotide sequence surrounding L^{74} is provided. This plasmid was mutagenized with primer 1 or 2 (the lower-case lettering represents base alterations in the nucleotide sequence from [$K2_{tPA}/W^{74}L$]), resulting in plasmids pSTII[$K2_{tPA}/W^{74}F$] and pSTII[$K2_{tPA}/W^{74}Y$], which are direct *E. coli* expression vectors for r-SD[$K2_{tPA}/W^{74}F$]S and r-SD[$K2_{tPA}/W^{74}Y$]S, respectively. PhoA refers to the alkaline phosphatase promoter region, stII represents the heat-stable enterotoxin signal sequence, and x symbolizes a stop codon.

maximal intrinsic fluorescence alteration accompanying binding of these ligands to wtr-[$K2_{tPA}$] (De Serrano et al., 1991), which is similar to ligand-induced intrinsic fluorescence changes in r-[$K1_{HPg}$] (Menhart et al., 1991), r-[$K4_{HPg}$] (Novokhatny et al., 1989), and r-[$K5_{HPg}$] (Novokhatny et al., 1989). Intrinsic fluorescence changes also accompanied binding of EACA and 7-AHpA to the variants produced in this work. The magnitudes of the changes observed were dependent on the particular variant and ligand investigated. For wtr-[$K2_{tPA}$] and r-[$K2_{tPA}/W^{74}L$], positive intrinsic fluorescence changes occurred at 25 °C and ranged from a maximum of 16% for the r-[$K2_{tPA}/W^{74}L$]/EACA interaction to 28% for the r-[$K2_{tPA}$]/EACA interaction. Negative intrinsic fluorescence changes were found to result from interaction of these ligands with r-[$K2_{tPA}/W^{74}S$] and r-[$K2_{tPA}/W^{74}F$], which at 25 °C ranged from a maximum of −7.6% for the r-[$K2_{tPA}/W^{74}F$]/EACA complex to −31% for the interaction of r-[$K2_{tPA}/W^{74}S$] with 7-AHpA. On the other hand, only very small fluorescence alterations occurred at 25 °C upon binding of these same ligands to r-[$K2_{tPA}/W^{74}Y$]. However, a decrease of the temperature to 10 °C led to maximal fluorescence alteratinos of −8.9% and −13.7%, respectively, upon complex formation with EACA and 7-AHpA. All of the above intrinsic fluorescence alterations were readily titratable with the appropriate ligand, and an example of the

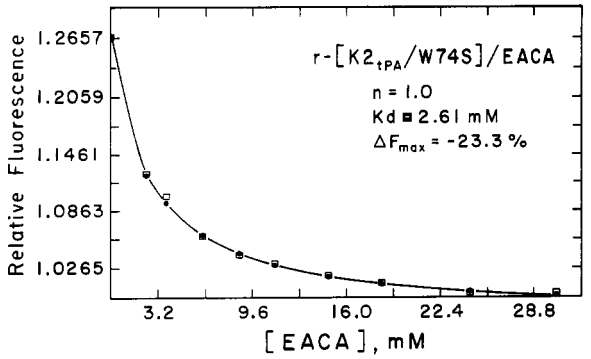

FIGURE 3: Titration of the change in relative intrinsic fluorescence of r-[$K2_{tPA}$/W^{74}S] (6.95 μM) with EACA. The experimental points (□) are best-fitted to a line (●) generated by employing values of n = 1.0, K_d = 2.61 mM, and a maximal relative fluorescence change (ΔF_{max}) of −23.3%. The buffer was 50 mM Tris–OAc/150 mM NaOAc, pH 8.0, at 25 °C. The excitation and emission wavelengths were 285 and 340 nm, respectively.

Table II: Binding Constants of ω-Amino Acids to W^{74} Mutants of the Recombinant Kringle 2 Region of Tissue-Type Plasminogen Activator As Determined by Intrinsic Fluorescence Titrations

	K_d (μM) for [a]				
ligand	wt	W^{74}S	W^{74}L	W^{74}F	W^{74}Y
EACA	42 ± 6	2780 ± 250	9700 ± 700	472 ± 35	1016 ± 95
7-AHpA	6 ± 2	1800 ± 140	3400 ± 250	113 ± 11	307 ± 23

[a] The temperature was 25 °C for all kringles except W^{74}Y, the binding data for which was obtained at 10 °C.

Table III: Binding Constants of ω-Amino Acids to W^{74} Mutants of the Recombinant Kringle 2 Region of Tissue-Type Plasminogen Activator As Determined by Titration Calorimetry at 25 °C

	K_d (μM) for		
ligand	wt	W^{74}F	W^{74}Y
EACA	35 ± 5	479 ± 30	821 ± 85
7-AHpA	9 ± 2	195 ± 15	248 ± 20

data from such an experiment with r-[$K2_{tPA}$/W^{74}S] titrated with EACA is illustrated in Figure 3. The K_d values, determined as previously described (Menhart et al., 1991), for all variants employed in this investigation are listed in Table II. The fact that binding data for ligands with r-[$K2_{tPA}$/W^{74}Y] were obtained at 10 °C does not raise a serious problem in comparison, since temperature responses to ligand binding over this range are not large. For example, when the same binding of 7-AHpA to r-[$K2_{tPA}$/W^{74}F] was analyzed at 10 °C, K_d values of 86–100 μM were obtained, as compared to an average K_d of 113 μM, at 25 °C (Table II).

A second procedure, titration calorimetry, was used to confirm the K_d values obtained by the above fluorescence technique. We have previously employed this latter method successfully to measure ω-amino acid ligand binding to [$K4_{HPg}$] (Sehl & Castellino, 1990) and to r-[$K1_{HPg}$] (Menhart et al., 1991). An example of a titration of r-[$K2_{tPA}$/W^{74}F] with EACA is presented in Figure 4. Calorimetric titrations were performed with EACA and 7-AHpA, at 25 °C, with wtr-[$K2_{tPA}$], as well as with its W^{74}F and W^{74}Y variants. In deconvoluting the data, the value of n (the stoichiometry of the ligand/kringle complexes) was set at 1.0 (Cleary et al., 1989), which improved the accuracy of the K_d calculation. This approach is justified since these kringles were purified by an affinity chromatography procedure which only provides molecules containing the ω-amino acid binding site. A summary of the data obtained is provided in Table III. This method could not be employed for the other two variants, i.e.,

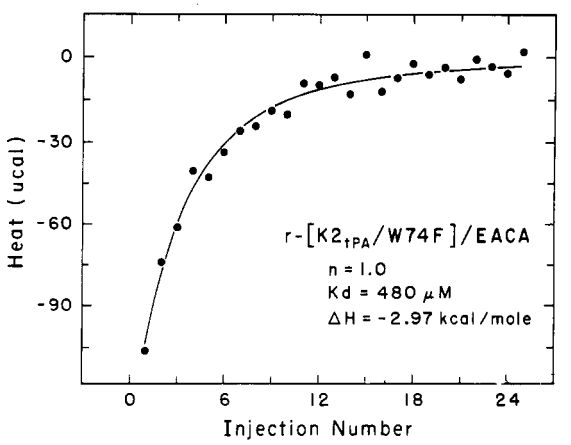

FIGURE 4: Titration of the heat of reaction of r-[$K2_{tPA}$/W^{74}F] with EACA. An automated sequence of aliquots (2 μL) of a stock solution (80 mM) of EACA was injected into a 0.159 mM solution of r-[$K2_{tPA}$/W^{74}F], and the heat changes were recorded. The data (●) were deconvoluted and best-fit to the line representing a binding isotherm with values of n = 1.0, K_d = 480 μM, and ΔH = −2.97 kcal/mol. The buffer was 50 mM Tris–OAc/150 mM NaOAc, pH 8.0, at 25 °C.

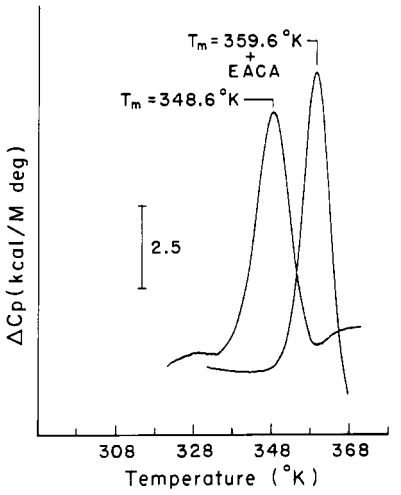

FIGURE 5: DSC thermograms of r-[$K2_{tPA}$] and the r-[$K2_{tPA}$]/EACA complex. The change in heat capacity at constant pressure (ΔC_p) is plotted against the temperature. The buffers employed were 50 mM Tris–OAc/150 mM NaOAc, pH 8.0, or 50 mM Tris–OAc/100 mM NaOAc/50 mM EACA, pH 8.0. The temperature of maximum heat capacity (T_m) for each sample is indicated on the graph.

r-[$K2_{tPA}$/W^{74}L] and r-[$K2_{tPA}$/W^{74}S], since ligand binding was too weak to be accurately determined by this method. It is clear from comparison of Tables II and III that these two disparate methods provided very similar K_d values.

In order to evaluate whether W^{74} of r-[$K2_{tPA}$] was important to the stability of this domain, we have evaluated the thermal denaturation properties of the wild-type polypeptide and compared its thermal stability with the various W^{74} mutants prepared for this investigation. An example DSC thermogram for wtr-[$K2_{tPA}$] is illustrated in Figure 5. The temperature of maximum heat capacity (T_m) is approximately 75.4 °C (348.6 K), which is raised to 86.4 °C (359.6 K) in the presence of sufficient EACA to saturate the binding site for this ligand. This significant stabilization of the native structure (or generation of a new and more stable conformation of the kringle) of wtr-[$K2_{tPA}$] resulting from ligand binding was first observed for [$K4_{HPg}$] and [$K5_{HPg}$] (Castellino et al., 1981) and later for r-[$K1_{HPg}$] (Menhart et al., 1991). Similar experiments have been performed with the variant kringles, and the T_m values obtained are listed in Table IV. In all cases examined,

Table IV: Thermal Stabilities of W^{74} Variants of the Recombinant Kringle 2 Domain of Tissue-Type Plasminogen Activator

variant	T_m[a] (°C) (−EACA)[b]	T_m[a] (°C) (+EACA)[c]
wt	75.4 ± 0.3	86.4 ± 0.4
$W^{74}S$	73.7 ± 0.3	76.5 ± 0.3
$W^{74}L$	71.7 ± 0.3	73.9 ± 0.4
$W^{74}F$	71.9 ± 0.4	81.2 ± 0.4
$W^{74}Y$	73.0 ± 0.3	81.6 ± 0.4

[a] Temperature of maximum heat capacity change. [b] The buffer was 50 mM Tris–OAc/150 mM NaOAc, pH 8.0. [c] The buffer was 50 mM Tris–OAc/100 mM NaOAc/50 mM EACA, pH 8.0.

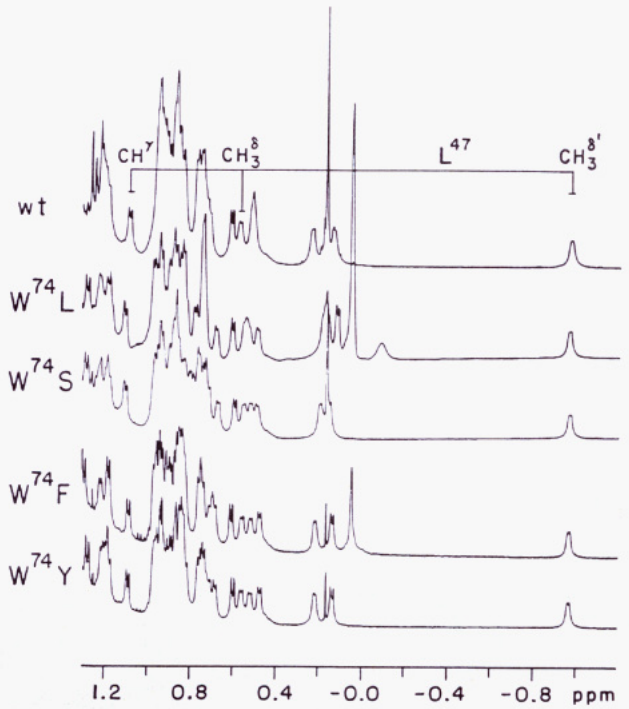

FIGURE 6: Methyl region of the ^{1}H-NMR spectra of wtr-[$K2_{tPA}$] and its W^{74} variants: viz., wtr-[$K2_{tPA}$]; r-[$K2_{tPA}/W^{74}L$]; r-[$K2_{tPA}/W^{74}S$]; r-[$K2_{tPA}/W^{74}F$]; r-[$K2_{tPA}/W^{74}Y$]. The CH_3^{δ}, $CH_3^{\delta'}$, and CH proton resonances from L^{47}, obtained from RELAYED-COSY experimentation, are indicated on the wtr-[$K2_{tPA}$] spectrum. The temperature was 37 °C and the pH* was 7.4.

substitution of W^{74} led to a slight lowering of the T_m value, indicating that only a minor structural destabilization occurred. The $W^{74}F$ and $W^{74}Y$ variants responded to EACA binding in a manner similar to that of their wild-type counterpart (Table IV). Interestingly, despite saturation of the EACA binding site in the $W^{74}L$ and $W^{74}S$ mutants, the T_m values were only increased by 2–3 °C, indicating that this ligand does not stabilize the native structures (or lead to significantly more stabilized alternate conformations) of these variants to the same extent as wtr-[$K2_{tPA}$] or its $W^{74}F$ and $W^{74}Y$ mutants.

The ^{1}H-NMR spectra of the high-field (−1 ppm < δ < 1.3 ppm) methyl region of wtr-[$K2_{tPA}$], and the variants employed in this study, are presented in Figure 6. Importantly, two COSY-connected doublets at approximately −1 ppm and approximately 0.55 ppm, arising from the CH_3^{δ} and $CH_3^{\delta'}$ side chains of L^{47} (Byeon et al., 1989), appear in all of the spectra. The exact chemical shifts of these resonances are listed in Table V.

Figure 7 illustrates the ^{1}H-NMR spectra of the aromatic region (5.0 ppm < δ < 8.5 ppm) of wtr-[$K2_{tPA}$], and its two aromatic variants, viz., r-[$K2_{tPA}/W^{74}F$] and wtr-[$K2_{tPA}/W^{74}Y$], employed in this investigation. From these spectra and related COSY connectivities, we have been able to assign all proton resonances of the mutated residues, with the assistance of previously assigned W^{74} resonances in wtr-[$K2_{tPA}$] (Byeon et al., 1989). The F^{74} resonances in r-[$K2_{tPA}/W^{74}F$]

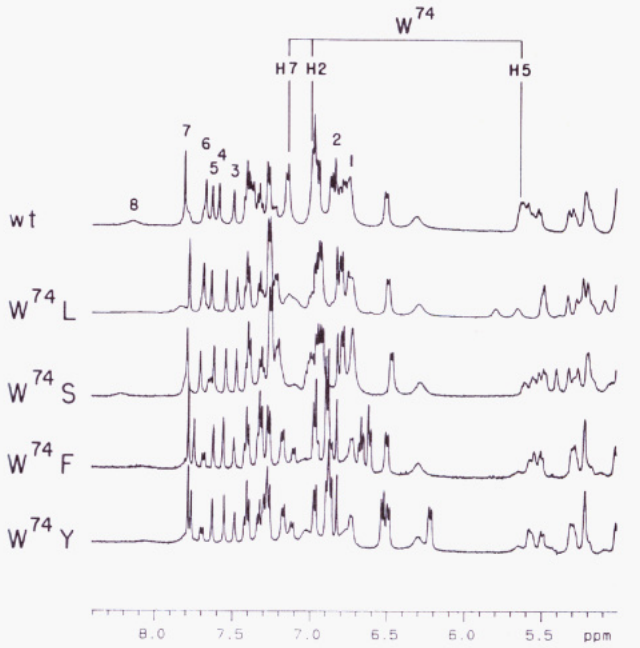

FIGURE 7: Aromatic region of the ^{1}H-NMR spectra of [$K2_{tPA}$] and its W^{74} variants: viz., wtr-[$K2_{tPA}$]; r-[$K2_{tPA}/W^{74}L$]; r-[$K2_{tPA}/W^{74}S$]; r-[$K2_{tPA}/W^{74}F$]; r-[$K2_{tPA}/W^{74}Y$]. Singlet proton resonances in wtr-[$K2_{tPA}$] arising from H and W residues are numbered 1 through 8, from lower to higher field: peak 8, H^{65} (H2); peak 7, H^{13} (H2); peak 6, W^{63} (H2); peak 5, H^{50} (H2); peak 4, H^{13} (H4); peak 3, W^{25} (H2); peak 2, H^{50} (H4); peak 1, H^{65} (H4). The H7, H2, and H5 resonances from W^{74} are indicated on the wtr-[$K2_{tPA}$] spectrum. The temperature was 37 °C and the pH* was 7.4.

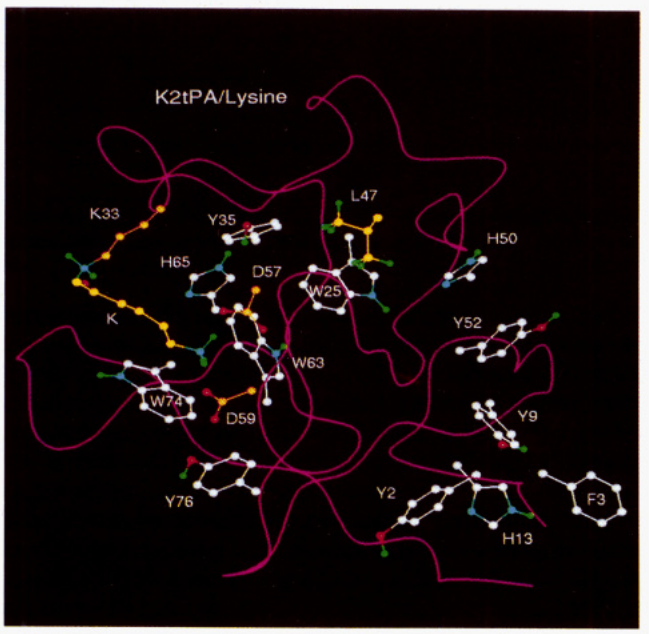

FIGURE 8: X-ray structure of wtr-[$K2_{tPA}$]. Selected amino acid side chains are displayed on the backbone structure, as indicated. The numbering of amino acids begins at C^1 of the r-[$K2_{tPA}$] sequence and continues consecutively without gaps or insertions. Each amino acid is displayed from its β-carbon (most hydrogen atoms are excluded to minimize overcrowding). The backbone conformation is in magneta. Hydrophobic amino acid side-chain carbon atoms (including those from H residues) are in white, charged amino acid side-chain carbons are in orange, nitrogen atoms are in blue, oxygen atoms are in red, and hydrogen atoms are in green. In order to highlight the lysine (K) inserted into the binding pocket and the side chain of L^{47}, the side-chain carbon atoms are in yellow.

Table V: ^{1}H-NMR Methyl Resonances for L^{47} at pH* 7.4 and 37 °C

variant	CH_3^{δ} δ (ppm)	$CH_3^{\delta'}$ δ (ppm)
wt	−0.964, −0.971	0.564, 0.574
$W^{74}L$	−0.959, −0.966	0.520[a]
$W^{74}S$	−0.960, −0.969	0.547, 0.555
$W^{74}F$	−0.962, −0.971	0.552, 0.563
$W^{74}Y$	−0.961, −0.972	0.554, 0.566

[a] Poorly resolved doublet.

Table VI: ^{1}H-NMR Aromatic Proton Resonances at Position 74 of r-[$K2_{tPA}$] and Its Aromatic Residue Variants at pH* 7.4 and 37 °C

sample	proton	δ (ppm)	sample	proton	δ (ppm)
wt, W^{74}	H2 (s)[a]	6.893	$W^{74}F$	H3,5 (t)[c]	6.956
	H4 (d)[b]	6.806		H4 (t)[c]	6.663
	H5 (t)[c]	5.611		H2,6 (d)[b]	6.608
	H6 (t)[c]	6.784	$W^{74}Y$	H2,6 (d)[b]	6.523
	H7 (d)[b]	7.144		H3,5 (d)[b]	6.216

[a] s, singlet. [b] d, doublet. [c] t, triplet.

Table VII: W^{74} Mutation Induced Shifts of Aromatic Proton Resonances of r-[$K2_{tPA}$] at pH* 7.4 and 37 °C

	Δδ (×10^3 ppm) for						
	H^{13}		H^{50}		H^{65}	W^{25}	W^{63}
variant	H2	H4	H2	H4	H2	H2	H2
$W^{74}L$	−35	−51	+1	−12	+35	−27	+10
$W^{74}S$	−15	−41	−7	−7	+83	−12	+39
$W^{74}F$	−31	−33	−12	−12	−77	−7	+70
$W^{74}Y$	−28	−40	−4	−11	−87	−10	+89

can be readily observed in the spectrum. The expected triplet for the H3,5 protons appears at approximately 6.96 ppm, the H4 triplet occurs at approximately 6.66 ppm, and the H2,6 doublet is observed at approximately 6.61 ppm. In the case of Y^{74} in r-[$K2_{tPA}/W^{74}Y$], a new H2,6 doublet appears at approximately 6.53 ppm and the doublet for the H3,5 protons occurs at approximately 6.21 ppm. In the cases of both of these variants, the appropriate proton resonances for W^{74} disappear. A listing of the exact proton resonances at amino acid sequence position 74 for these recombinant kringles is provided in Table VI. Chemical shift differences, as compared to wtr-[$K2_{tPA}$], of some other clearly assignable proton resonances present in the variant kringles are listed in Table VII.

Discussion

On the basis of NMR investigations with the ω-amino acid-binding kringles, [$K1_{HPg}$] (Motta et al., 1987), [$K4_{HPg}$] (Ramesh et al., 1987), [$K5_{HPg}$] (Thewes et al., 1990), and [$K2_{tPA}$] (Byeon et al., 1989), as well as molecular modeling of kringle domains (De Serrano et al., 1991; Sehl, 1991), and X-ray crystallographic investigation of wtr-[$K2_{tPA}$][2] (de Vos et al., 1992) and [$K4_{HPg}$][3] (Mulichak et al., 1989), it appears as though a number of aromatic residues are involved in critical active site interactions with ligands of this type. Among the most notable of these residues is believed to be W^{74} in [$K2_{tPA}$] and the homologous residues Y^{71} present in [$K1_{HPg}$], W^{70} [$K4_{HPg}$], and Y^{72} in [$K5_{HPg}$]. In the current investigation, we have directly determined by generation of nonconservative recombinant variants of [$K2_{tPA}$], i.e., $W^{74}L$ and $W^{74}S$, that W^{74} in r-[$K2_{tPA}$] plays a crucial role in the binding of ω-amino acid ligands to this kringle domain (Tables III and IV). In addition, although more conservative aromatic amino acid substitutions, i.e., $W^{74}F$ and $W^{74}Y$, are tolerated in terms of this binding (Tables II and III), W, positioned at amino acid sequence position 74, is by far the most effective amino acid in stabilizing this binding interaction.

While some local structural alterations probably occur as a result of the W^{74} mutations, our evidence shows that gross conformational integrity of wtr-[$K2_{tPA}$] is maintained in the variant forms of this kringle. From DSC analysis of the thermal stability of the various kringles, we conclude that the variants exhibit melting behavior similar to that of the wild-type counterpart. Some destabilization of the structure does occur in all cases, most notably in the $W^{74}L$ and $W^{74}F$ variants, but this is not large and we conclude that W^{74} is not an amino acid residue that is critical for maintenance of the structural stability of r-[$K2_{tPA}$]. More interesting, however, is the effect of EACA on the thermal stability of this kringle domain. At sufficient levels of EACA to saturate its binding site on all of the recombinant kringles used in this work, the T_m for wtr-[$K2_{tPA}$], r-[$K2_{tPA}/W^{74}F$], and r-[$K2_{tPA}/W^{74}Y$] increased by 8–11 °C, demonstrating a substantial stabilizing effect on the native conformation of these kringles or generation of a new and more stable conformation. However, for r-[$K2_{tPA}/W^{74}L$] and r-[$K2_{tPA}/W^{74}S$], despite the fact that EACA was present at concentrations at least 5-fold greater than the K_d for this ligand (≥82% saturation), only a small increase (ca. 2–3 °C) in the T_m of the kringle occurred. This could be due to altered binding interactions between these latter variant kringles and the ligand and/or an altered thermal denaturation mechanism. An example of the latter would involve a temperature-induced dissociation of the ligand from its binding site prior to the thermal unfolding of the kringle, an event which may result from the weaker interactions of EACA with the $W^{74}L$ and $W^{74}S$ variants.

The ^{1}H-NMR spectra of the wild-type kringle and the W^{74} variants generated herein, illustrating the methyl proton region and the aromatic proton area, are shown in Figures 6 and 7, respectively. There is a wide spectral dispersion of protons in each case, suggesting that all kringles are folded and globular. Of great importance, the high-field proton doublet that resonates at approximately −1 ppm, arising from the ring current shift of $CH_3^{\delta'}$ protons of L^{47} in close contact with the aromatic ring of W^{25}, is present in each case. From two-dimensional COSY connectivities, we have identified the CH_3^{δ} doublet resonance from that same leucine residue at approximately 0.55–0.57 ppm (Table V). Protons from both CH_3 groups of L^{47} have been found to possess scalar connectivity to a CH^{γ} of this same L residue, present as a multiplet split by each of the nonidentical CH_3 protons. The resonance positions of the unresolved multiplet are present at approximately 1.1 ppm in the case of all variants. This large difference in chemical shift of the protons from apparently equivalent methyl groups, a very sensitive marker of overall proper kringle folding (DeMarco et al., 1982; Thewes et al., 1978; Byeon et al., 1990), strongly suggests that all variant kringles are folded similarly to their wild-type counterpart.

While it is not possible to make a detailed analysis of mutated kringle conformations from the ^{1}H-NMR spectra of Figure 7, and the related COSY analyses, the spectral data that we have obtained, in conjunction with the resonance assignments made earlier (Byeon et al., 1989), do allow some observations to be made concerning the effect of W^{74} substitutions on the chemical environments of other residues in the [$K2_{tPA}$] domain. To enhance this discussion, we have provided our graphical construction[4] of the X-ray structure

[3] The coordinates were provided to this laboratory by Dr. Alexander Tulinsky, Michigan State University, East Lansing, MI.

[4] B. A. K. Chibber and F. J. Castellino, unpublished data.

of the [$K2_{tPA}$] domain in Figure 8 (de Vos et al., 1992), with selected amino acids displayed.

From the ^{1}H-NMR spectra of Figure 7, we observe that the proton resonances from the CH_3^{δ} and $CH_3^{\delta'}$ protons of L^{47} are in nearly the same locations as present in the wild-type kringle in all of the variants. This is especially significant in the case of the high-field $CH_3^{\delta'}$ doublet, since this resonance position is governed by the close interaction of this methyl group with the aromatic ring of W^{25} (Figure 8). Thus, in addition to the calorimetric evidence presented, this aspect of the ^{1}H-NMR data shows that gross conformational differences between the wtr-[$K2_{tPA}$] and any of the variant forms of this kringle domain investigated here are unlikely.

For those amino acid residues showing low-field singlet proton resonances, the data of Figure 7 and Table VII show that the largest chemical shift differences in the mutant forms of r-[$K2_{tPA}$], as compared to the resonances in wtr-[$K2_{tPA}$], are found for the H2 and H4 protons of H^{13}, the H2 proton of H^{65}, and the H2 proton of W^{63}. The most important differences are found in the environment of W^{63}, which forms one hydrophobic wall of the binding site for ω-amino acids (Figure 8) and is sufficiently proximal to W^{74} to be directly influenced by mutations at that position (Figure 8). While the absence of W^{74} in the W^{74}L and W^{74}S mutants is likely responsible for the very weak binding of ω-amino acids to these mutants, the environmental alteration that occurs in W^{63}, in the W^{74}F and W^{74}Y variants, may well explain their diminished binding to 7-AHpA and EACA, as compared to the wtr-[$K2_{tPA}$]. Regarding H^{13}, this residue is not in the vicinity of W^{74} in wtr-[$K2_{tPA}$], and alterations in its environment as a result of the mutations at W^{74} suggest that this residue is in long-range communication with a residue(s) directly influenced by changes at W^{74}. Unless a large conformational alteration occurred in the particular variants employed herein, for which calorimetric and NMR evidence provides evidence to the contrary, it is unlikely that the environmental alterations seen at H^{13} are responsible for the binding differences seen with the variants. On the other hand, H^{65} is sufficiently close to both W^{74} and W^{63} to be influenced by changes in these residues, but H^{65} has been shown to play only a minor role in binding of wtr-[$K2_{tPA}$] to ω-amino acids (Kelley & Cleary, 1989). Therefore, it is unlikely that the environmental alterations observed at H^{65}, as a result of the mutations, are significant in regard to the substantially weaker binding displayed by the W^{74}-variant forms of r-[$K2_{tPA}$]. Much smaller changes are also found in the H2 and H4 resonances of H_{50}, and the H2 resonance of W^{25}, indicating that these perturbations are not of major significance. The proton signals from aromatic residues not substantially affected by the mutations at W^{74} include the H2,6 doublet of Y^2 and the H2,6 doublet of Y^{52} ($\Delta\delta < 0.01$ ppm). These results suggest that these two residues do not communicate with W^{74}.

It is clear from the X-ray structure (Figure 8) that D^{57} and D^{59} may be very important to the stability of the [$K2_{tPA}$]/ω-amino acid interaction. It is possible that the mutations constructed have affected their geometries, thereby influencing binding. Since the positions of these residues in the NMR spectrum have not been assigned, this point cannot be rigorously evaluated. However, if such an event has occurred, it must be very subtle, since gross conformational changes in r-[$K2_{tPA}$] have not accompanied the mutations described.

In summary, we have shown that nonaromatic mutations at W^{74} of the isolated r-[$K2_{tPA}$] domain of tPA virtually eliminate its ability to interact with ω-amino acids. Aromatic substitutions are more readily tolerated at this position but still do not restore the wild-type kringle binding properties. Thus, a W residue at this location is critical to this binding interaction. While some degree of localized conformational alterations in the W^{74}F and W^{74}Y mutants, especially at W^{63}, may contribute to the diminished binding properties of the variant kringles, there do not appear to be gross conformational changes in these mutant kringles that are of sufficient magnitude to explain the large loss of binding stabilization. Thus, W^{74} is directly implicated in the binding stabilization energy. Finally, W^{74} is not critical for the stability of the proper kringle conformation, since none of the substitutions made at this location significantly destabilized this polypeptide.

References

Byeon, I.-J. L., Kelley, R. F., & Llinas, M. (1989) *Biochemistry 28*, 9350–9360.

Castellino, F. J., Ploplis, V. A., Powell, J. R., & Strickland, D. K. (1981) *J. Biol. Chem. 256*, 4778–4782.

Chang, C. N., Rey, M., Bochner, B., Heyneker, H., & Gray, G. (1987) *Gene 55*, 189–196.

Cleary, S., Mulkerrin, M. G., & Kelley, R. F. (1989) *Biochemistry 28*, 1884–1891.

DeMarco, A., Hochschwender, S. M., Laursen, R. A., & Llinas, M. (1982) *J. Biol. Chem. 257*, 12716–12721.

DeMarco, A., Motta, A., Llinas, M., & Laursen, R. A. (1985) *Biophys. J. 48*, 411–422.

DeMarco, A., Petros, A. M., Laursen, R. A., & Llinas, M. (1987) *Eur. Biophys. J. 14*, 359–368.

DeMarco, A., Petros, A. M., Llinas, M., Kaptein, R., & Boelens, R. (1989) *Biochim. Biophys. Acta 994*, 121–137.

de Munk, G. A. W., Caspers, M. P. M., Chang, G. T. G., Pouwels, P. H., Enger-Valk, B. E., & Verheijen, J. H. (1989) *Biochemistry 28*, 7318–7325.

De Serrano, V. S., & Castellino, F. J. (1990) *J. Biol. Chem. 265*, 10473–10478.

De Serrano, V. S., Sehl, L. C., & Castellino, F. J. (1991) *Arch. Biochem. Biophys. 292*, 206–212.

De Serrano, V. S., Menhart, N., & Castellino, F. J. (1992) *Arch. Biochem. Biophys.* (in press).

de Vos, A. M., Ultsch, M. H., Kelley, R. F. Padmanabhan, K., Tulinsky, A., Westbrook, M. L., & Kossiakoff, A. A. (1992) *Biochemistry 31*, 270–279.

Eich, G., Bodenhausen, G., & Ernst, R. R. (1982) *J. Am. Chem. Soc. 104*, 3731–3732.

Kelley, R. F., & Cleary, S. (1989) *Biochemistry 28*, 4047–4054.

Kurecki, T., Kress, L. F., & Laskowski, M., Sr. (1979) *Anal. Biochem. 99*, 415–420.

Laemmli, U. K. (1970) *Nature (London) 227*, 680–685.

Lech, K., & Brent, R. (1987) in *Current Protocols in Molecular Biology* (Ausubel, F. M., Brent, R., Kingston, R. E., Moore, D. D., Seidman, J. G., Smith, J. A., & Struhl, K., Eds.) pp 1.6.1–1.6.10, John Wiley & Sons, New York, NY.

Lerch, P. G., Rickli, E. E., Lergier, W., & Gillessen, D. (1980) *Eur. J. Biochem. 107*, 7–13.

Magnusson, S., Petersen, T. E., Sottrup-Jensen, L., & Claeys, H. (1975) in *Proteases and Biological Control* (Reich, E., Rifkin, D. B., & Shaw, E., Eds.) pp 123–149, Cold Spring Harbor Laboratories, Cold Spring Harbor, NY.

Markus, G., DePasquale, J. L., & Wissler, F. C. (1978a) *J. Biol. Chem. 253*, 727–732.

Markus, G., Evers, J. L., & Hobika, G. (1978b) *J. Biol. Chem. 253*, 733–739.

McLean, J. W., Tomlinson, J. E., Kuang, W.-j., Eaton, D. L., Chen, E. Y., Gless, G. M., Scanu, A. M., & Lawn, R. M.

(1987) *Nature (London) 330*, 132-137.
McMullen, B. A., & Fujikawa, K. (1985) *J. Biol. Chem. 260*, 5328-5341.
Menhart, N., Sehl, L. C., Kelley, R. F., & Castellino, F. J. (1991) *Biochemistry 30*, 1948-1957.
Miles, L. A., Dahlberg, C. M., & Plow, E. F. (1988) *J. Biol. Chem. 263*, 11928-11934.
Motta, A., Laursen, R. A., Rajan, N., & Llinas, M. (1986) *J. Biol. Chem. 261*, 13684-13692.
Motta, A., Laursen, R. A., Tulinsky, A., & Park, C. H. (1987) *Biochemistry 26*, 3827-3836.
Mulichak, A. M., Park, C. H., Tulinsky, A., Petros, A. M., & Llinas, M. (1989) *J. Biol. Chem. 264*, 1922-1923.
Novokhatny, V. V., Matsuka, Y. V., & Kudinov, S. A. (1989) *Thromb. Res. 53*, 243-252.
Pennica, D., Holmes, W. E., Kohr, W. J., Harkins, R. N., Vehar, G. A., Ward, C. A., Bennett, W. F., Yelverton, E., Seeburg, P. H., Heyneker, H. L., Goeddel, D. V., & Collen, D. (1983) *Nature (London) 301*, 214-221.
Radek, J. T., & Castellino, F. J. (1988) *Arch. Biochem. Biophys. 267*, 776-786.
Ramesh, V., Petros, A. M., Llinas, M., Tulinsky, A., & Park, C. H. (1987) *J. Mol. Biol. 198*, 481-498.
Sanger, F. Nicklen, S., & Coulson, A. R. (1977) *Proc. Natl. Acad. Sci. U.S.A. 74*, 5463-5467.
Sehl, L. C. (1991) Ph.D. Dissertation, University of Notre Dame.
Sehl, L. C., & Castellino, F. J. (1990) *J. Biol. Chem. 265*, 5482-5486.
Seidman, C. E. (1987) in *Current Protocols in Molecular Biology* (Ausubel, F. M., Brent, R., Kingston, R. E., Moore, D. D., Seidman, J. G., Smith, J. A., & Struhl, K., Eds.) pp 1.8.1-1.8.3, John Wiley & Sons, New York, NY.
Sottrup-Jensen, L., Claeys, H., Zajdel, M., Petersen, T. E., & Magnusson, S. (1978) *Prog. Chem. Fibrinolysis Thrombolysis 3*, 191-209.
Steffens, G. J., Gunzler, W. A., Otting, F., Frankus, E., & Flohe, L. (1982) *Hoppe-Seyler's Z. Physiol. Chem. 363*, 1043-1058.
Thewes, T., Ramesh, V., Simplaceanu, E. L., & Llinas, M. (1987) *Biochim. Biophys. Acta 912*, 254-269.
Thewes, T., Constantine, K., Byeon, I.-J. L., & Llinas, M. (1990) *J. Biol. Chem. 265*, 3906-3915.
Thorsen, S. (1975) *Biochim. Biophys. Acta 393*, 55-65.
Thorsen, S., Clemmensen, J., Sottrup-Jensen, L., & Magnusson, S. (1981) *Biochim. Biophys Acta 668*, 377-387.
Trexler, M., Vali, Z., & Patthy, L. (1982) *J. Biol. Chem. 257*, 7401-7406.
Tulinsky, A., Park, C. H., Mao, B., & Llinas, M. (1988) *Proteins: Struct, Funct., Genet. 3*, 85-96.
Vali, Z., & Patthy, L. (1984) *J. Biol. Chem. 259*, 13690-13694.
van Zonneveld, A.-J., Veerman, H., & Pannekoek, H. (1986) *Proc. Natl. Acad. Sci. U.S.A. 83*, 4670-4674.
Vieira, J., & Messing, J. (1987) *Methods Enzymol. 153*, 3-11.
Wiman, B., & Wallen, P. (1977) *Thromb. Res. 10*, 213-222.
Wiman, B., & Collen, D. (1978) *Nature (London) 272*, 549-550.

The YF161D1 Mutant of *Synechocystis* 6803 Exhibits an EPR Signal from a Light-Induced Photosystem II Radical†

G. H. Noren and B. A. Barry*
Department of Biochemistry, University of Minnesota, St. Paul, Minnesota 55108
Received October 11, 1991; Revised Manuscript Received January 22, 1992

ABSTRACT: The currently accepted model for the location of the redox-active tyrosines, D and Z, in photosystem II suggests that they are symmetrically located on the D1 and D2 polypeptides, which are believed to form the heterodimer core of the reaction center. Z, the electron conduit from the manganese catalytic site to the primary chlorophyll donor, has been identified with tyrosine-161 of D1. The YF161D1 mutant of *Synechocystis* 6803 [Debus, R. J., Barry, B. A., Sithole, I., Babcock, G. T., & McIntosh, L. (1988b) *Biochemistry 27*, 9071-9074; Metz, J. G., Nixon, P. J., Rogner, M., Brudvig, G. W., & Diner, B. A. (1989) *Biochemistry 28*, 6960-6969], in which this tyrosine has been changed to a phenylalanine, should have no light-induced EPR (electron paramagnetic resonance) signal from a tyrosine radical. This negative result has indeed been obtained in analysis of one of two independently constructed mutants through the use of a non-oxygen-evolving core preparation (Metz et al., 1989). Here, we present an analysis of a YF161D1 mutant through the use of a photosystem II purification procedure that gives oxygen-evolving particles from wild-type *Synechocystis* cultures. In our mutant preparation, a light-induced EPR signal from a photosystem II radical is observed under conditions in which, in a wild-type preparation, we can accumulate an EPR signal from Z+. This EPR signal has a different lineshape from that of the Z+ tyrosine radical, and spin quantitation shows that this radical can be produced in up to 60% of the mutant reaction centers. The EPR lineshape of this radical suggests that photosystem II reaction centers of the YF161D1 mutant contain a redox-active amino acid.

In plants, algae, and cyanobacteria, photosystem II (PSII) catalyzes the light-induced oxidation of water and the reduction of plastoquinone. This photosystem is one of several membrane-associated protein complexes that carry out the initial electron-transfer events in oxygenic photosynthesis. PSII is a chlorophyll-containing complex that is composed of both integral, membrane-spanning polypeptides and extrinsic po-

† Supported by NIH Grant GM43272 and a McKnight-Land Grant award from the University of Minnesota to B.A.B.

0006-2960/92/0431-3335$03.00/0